Int. J. Heat Mass Transfer. Vol. 28, No. 1, pp. 235–243, 1985
Printed in Great Britain

0017–9310/85 $3.00 + 0.00

Measurements of true quench temperature of subcooled water under forced convective conditions

S. C. CHENG, P. W. K. LAU and K. T. POON
Department of Mechanical Engineering, University of Ottawa, Ottawa, Canada K1N 6N5

(*Received* 11 *July* 1983 *and in revised form* 29 *May* 1984)

Abstract—An experimental investigation was conducted to measure the true quench temperature using two hot patches to anchor quench fronts. The parametric effects of mass flux (range 50–682 kg m^{-2} s^{-1}), inlet subcooling (2–30°C), pressure (101–1034 kPa) and local quality (−0.0315–0.1990) are discussed. A correlation of true quench temperature in terms of parameters based on present experimental data was formulated. The measure true quench temperature is compared with those available from the literature. A special cold spot test series was conducted to examine the length effect on true quench temperature.

1. INTRODUCTION

FOLLOWING a postulated loss-of-coolant-accident in a water-cooled reactor, the lack of adequate cooling can result in dry-out occurring over a considerable part of the core. The fuel elements in dry-out will experience a significant rise in surface temperature. The establishment of adequate emergency core cooling will slowly lower these temperatures by precursory cooling, radiation and axial conduction. The injected water will only wet the fuel sheath when the surface temperature has been reduced to below the minimum film boiling temperature.

Determination of the minimum film boiling temperature is of great importance in reactor safety analysis. This minimum film boiling temperature separates the high temperature region, where inefficient film boiling or vapour cooling takes place, from the lower temperature region, where more efficient transition boiling occurs. It thus provides a limit to the application of transition boiling and film boiling correlations.

A large number of terms have been used to describe the phenomenon at the boundary between transition boiling and film boiling, e.g. rewetting, quenching, sputtering, DFFB (departure from film boiling), film boiling collapse, Leidenfrost phenomenon and minimum film boiling. A variety of correlations have been proposed to predict the corresponding temperature and heat flux. Unfortunately, none of these studied the onset of quench in the absence of a propagating rewetting front, so-called "true quench phenomenon" and the associated true quench temperature in the flow boiling situation.

The purpose of this study is to measure the true quench temperature and to investigate its parametric trends. The termination of the film boiling phenomenon encountered in this study is a result of the spontaneous collapse of a vapour film following a gradual reduction in the surface temperature. The experiments were performed on a single tube geometry with bottom flooding.

To anchor the quench front originated from both ends of the test section, a relatively new hot patch technique [1, 2] is used to establish steady-state film boiling for water during forced convection inside a directly heated channel.

Mechanisms

Two principal mechanisms have been proposed for the rewetting phenomenon:

(1) *Hydrodynamic mechanism.* The separation of the liquid–vapour interface from the wall can be maintained only as long as the vapour generation rate exceeds the vapour removal rate, i.e. vapour forces balance out liquid forces. If the fluid properties or the heated surface is changed to affect this vapour generation stability, then the vapour layer may collapse—hence rewetting.

Using the concept of Taylor Instability, Berenson [3] assumed that the Leidenfrost temperature would occur where vapour–liquid interface oscillations become unstable due to force imbalance. Such imbalance occurs when bubble spacing at the interface has reached the critical wavelength for which the amplitude of the disturbances (bubbles) grows most rapidly. Physically, the vapour–liquid interface is wavy, bubbles are released to the liquid at regular intervals, and liquid spikes form between the released bubbles sometimes wetting the heated surface.

(2) *Thermodynamic mechanism.* It is assumed that the liquid can never exist beyond a "maximum liquid temperature", which depends only on the liquid properties and hence is a unique function of pressure. Thus, a heated surface whose temperature is beyond the maximum liquid temperature cannot support liquid contact [4].

NOMENCLATURE

c	specific heat
G	mass flux
k	thermal conductivity
L	length
P	pressure
T	temperature
x	quality.

Greek symbols

ΔT	temperature difference
ρ	density.

Subscripts

crit	critical
l	liquid
liq	liquid
min	minimum
Q	quench
s	saturated
sat	saturated
sub	subcooled
w	wall.

2. TYPES OF REWETTING

Iloeje *et al.* [5] isolated three different controlling mechanisms for forced convective rewet. These are: impulse cooling collapse, axial conduction controlled rewet and dispersed flow rewet. Groeneveld [6] presented various types of rewetting as shown in Fig. 1. This figure includes the three controlling mechanisms mentioned above.

Forced convection rewet

(1) *Impulse cooling collapse.* At the wall temperature higher than the rewetting temperature in the inverted-annular vapour film boiling regime, the liquid–vapour interface is wavy and it fluctuates about a mean position. If the wall temperature or heat flux is lowered, the vapour thickness decreases and eventually the liquid may contact the wall. Depending on the temperature level and the rate of heat supply to the cooled region of material beneath the liquid, permanent liquid–wall contact is either maintained or the liquid is pushed away from the surface with the formation of vapour. In the latter case, each contact is equivalent to an impulsive cooling of the surface. In a quenching process, repeated contacts will lower the surface temperature enough to permit rewet. The type 1 of Fig. 1 shows the configuration of collapse of vapour film.

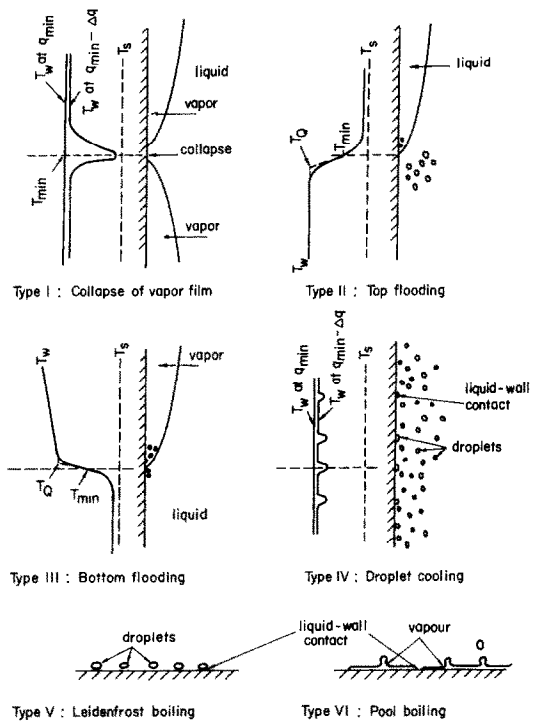

Type I : Collapse of vapor film
Type II : Top flooding
Type III : Bottom flooding
Type IV : Droplet cooling
Type V : Leidenfrost boiling
Type VI : Pool boiling

FIG. 1. Types of rewetting (Groeneveld [6]).

Kalinin *et al.* [7] performed a conduction analysis to obtain the temperature at the beginning and end of the film boiling crisis (i.e. the collapse of vapour film). The wall temperature corresponding to the minimum heat flux in forced convective flow can be obtained from their empirical correlation:

$$\frac{T_{\min}-T_{\text{sat}}}{T_{\text{crit}}-T_{\text{liq}}}=1.65\left\{0.1+0.6\frac{(\rho ck)_{\text{l}}}{(\rho ck)_{\text{w}}}+1.5\left[\frac{(\rho ck)_{\text{l}}}{(\rho ck)_{\text{w}}}\right]^{1/4}\right\}. \tag{1}$$

However, this model seems to be incomplete because the hydrodynamic parameter of the flow rate is completely absent.

Recently, the impulse cooling collapse type of rewetting has been studied by Groeneveld and Stewart [4] and Cheng *et al.* [8]. Preliminary correlations for the true quench temperature of this type of rewetting have been proposed by them.

(2) *Axial conduction controlled rewet.* In a system with an already wetted upstream surface, i.e. the type 2 and 3 configurations of Fig. 1, Simon and Simoneau [9] suggested that the transition from film boiling to nucleate boiling in an electrically heated system appeared to be governed by axial conduction. Wall conduction transfers the heat from the film boiling side to the nucleate boiling side and causes the surface temperature to drop as a function of time. Transition from film boiling to nucleate boiling occurs when the wall temperature at each position along the heating surface reaches the wetting temperature. Furthermore, Simon and Simoneau also assumed that the value of the wetting temperature corresponded to the maximum superheat of a fluid and this condition was determined by using the Van der Waals equation of state.

(3) *Dispersed flow rewet.* In the dispersed flow regime, Iloeje *et al.* [5] postulated that transition was

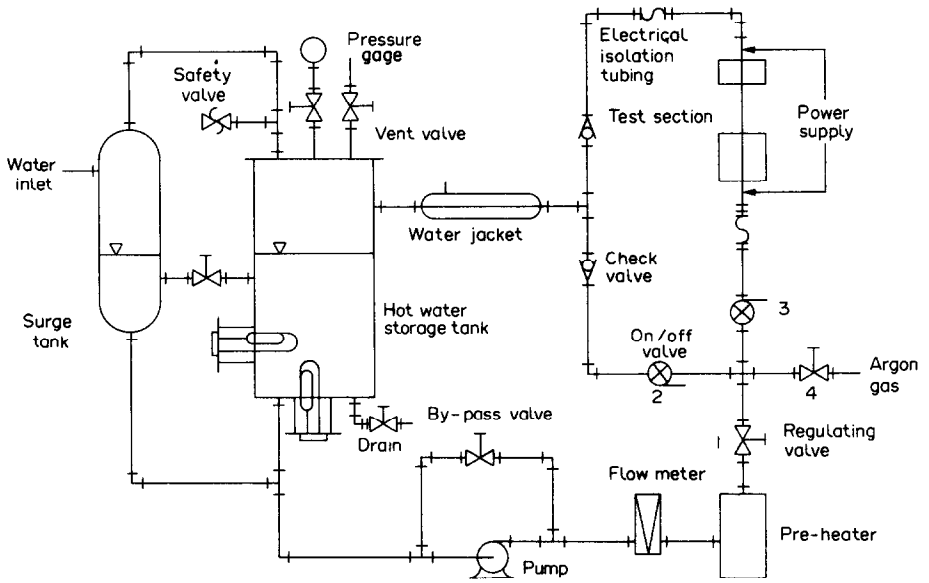

FIG. 2. Pressurized experimental loop.

controlled by the limiting effects of two processes; namely, heat transfer to the vapour assuming no effect of the existence of droplets, and heat transfer due to the presence of the droplets, which may or may not be touching the surface. The sum of the two heat transfer components gives the total heat flux and indicates the location of the minimum heat flux and ΔT_{min}.

Note that this is the type 4 of Fig. 1 rewetting characterized by the absence of a propagating rewetting front. It is thus similar to the type 1 film boiling configuration, except that the liquid phase is dispersed in the vapour instead of being continuous.

3. EXPERIMENTAL APPARATUS

There are two experimental loops involved in the experiments, one is an open loop operating at the atmospheric pressure and the other is a pressurized loop operating up to 1034 kPa [10]. Only the latter will be described in this paper.

The pressurized loop, as shown in Fig. 2, consists primarily of a 5 gallon surge tank, a 50 gallon hot water storage tank, a pump, a flow meter, a preheater, a test section and the associated valves and piping. Provisions of bypassing the pump and the test section were incorporated to stabilize the flow. The flow was circulated by a 1/4 hp pump, the flow rate was measured by a rotameter, and the flow adjustment was done via the regulatory needle valve 1. Valves 2 and 3 are on–off type which operate out-of-phase.

The system was pressurized by argon gas through the regulating valve 4, and the surge tank was used to moderate pressure variation. A solenoid vent valve was used to release the excess pressure during experiments. The system pressure value can be obtained from a pressure transducer and a voltmeter.

Test section assembly

A typical test section is shown schematically in Fig. 3. Its main component is an Inconel tube 91.4 cm long with o.d. varying from 1.27 to 1.31 cm and i.d. of 1.102 cm. To anchor the quench fronts originating from both ends of the test section, two copper hot patches, i.e. the bottom hot patch (BHP) and top hot patch (THP), were

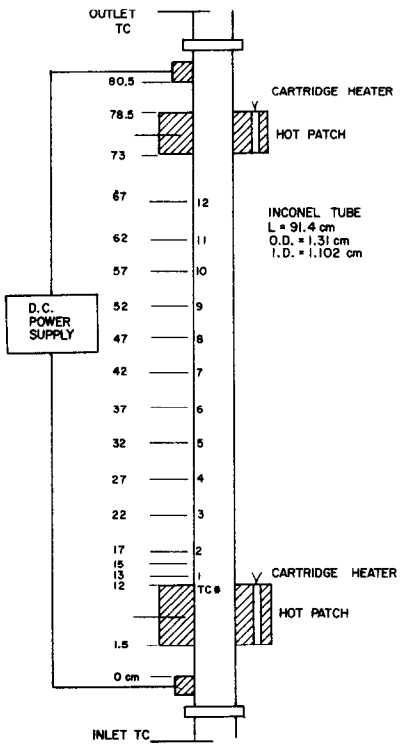

FIG. 3. Test section.

soldered to the Inconel tube using a high temperature silver solder (melting point at 780°C). Extra caution is required in the soldering process, otherwise the quench front could initiate from the hot patch. The BHP with 10.16 cm long was heated by eight 500 W cartridge heaters and the THP with 5.72 cm long by eight 250 W cartridge heaters. A thermocouple was embedded at the interface of the BHP and tube to be used for determining the film boiling curve of the BHP during a separate cool-down test of the BHP. About a dozen chromel–alumel thermocouples were spot welded onto the exterior of the tube at various axial locations as shown in Fig. 3. The entire test section assembly was insulated by high temperature ceramic fibre glass to reduce heat losses.

A Miller Welders direct current arc welder (40 V and 600 A) was employed as the test section direct power supply. Pirelli welding cable of 500 A capability was used to transmit power between the power supply and the test section.

4. EXPERIMENTAL PROCEDURE

(1) Water in the storage tank was heated to slightly below the desired test inlet temperature using immersion heaters which were thermostatically controlled. The system was then pressurized to the desired test pressure by injecting argon gas.

(2) The top and bottom hot patches were then heated to 500 and 700°C, respectively, well into the film boiling regime.

(3) The pump was turned on and the flow was first passed through the regulating valve 1, then through the on–off valve 2 (valve 3 closed), and drained back to the storage tank via the test section bypass loop.

(4) The preheater was used to raise the water temperature to the desired test inlet value.

(5) The Inconel tube was heated to about 700°C by the Miller Welders power supply with direct heating.

(6) The on–off valve 2 was closed and the on–off valve 3 opened to divert the flow into the test section.

(7) Starting from the tube temperature of 700°C, the power was reduced stepwise by approximately 5% each time. Sufficient time was allowed for the flow to stabilize between steps. The process was repeated until the first detection of true quench by thermocouples through chart recorders. The test was terminated when the tube started to rewet.

(8) For tests at high mass fluxes, sometimes it was necessary to start with a lower mass flux in order to prevent the test section from being quenched when the flow first reached it. The mass flux and the heat flux were then gradually increased to reach the desired flow rate.

(9) After each test run, argon gas was circulated through the Inconel tube to purge the residue liquid and to prevent oxidation at high heated surface temperature during the subsequent run.

5. EXPERIMENTAL RESULTS

Two run series were conducted for measurements of the true quench temperature, i.e. 10,200 run series at atmospheric pressure and 10,300 run series at higher pressures.

To calculate the local quality at the true quench location via energy balance, one must know the flow conditions, the heat flux of the test section through direct heating, the heat flux of the bottom hot patch and the heat losses of the test section. The first two are measurable during experiments. The determination of the heat flux of the BHP requires a separate cool-down test to obtain a film boiling curve from which the film boiling flux corresponding to the BHP temperature setting can be found [10]. Similarly, a separate test under a no-flow condition is required to determine heat losses of the test section. Some typical results for the 10,300 run series at $P = 344$ kPa are presented in Table 1 and also plotted in Figs 4 and 5 for studying parametric trends.

In general, for a fixed inlet subcooling (ΔT_{sub}) with increasing mass flux (G), the quench location moves downward towards the bottom hot patch as shown in

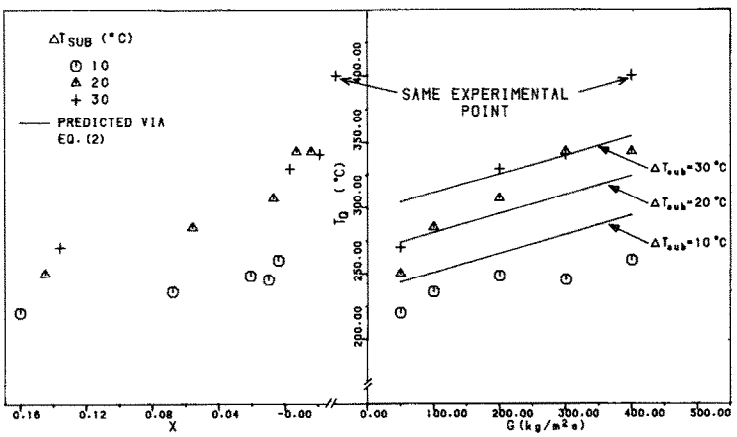

FIG. 4. Measured and predicted quench temperature vs mass flux and local quality for 10,300 run series at $P = 344$ kPa.

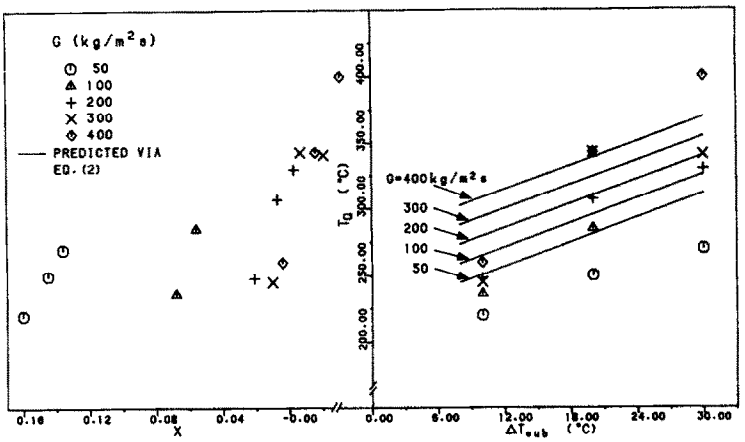

FIG. 5. Measured and predicted quench temperature vs inlet subcooling and local quality for 10,300 run series at $P = 344$ kPa.

Table 1. For increasing G, the heat transfer between the wall and the coolant becomes more efficient. The portion of tube adjacent to the BHP under the strong influence of hot patch temperature gradient diminishes, resulting in a downward movement of quench location. The observation of the effect of increasing ΔT_{sub} to the quench location exhibits a similar trend to that of the increase of G.

For a fixed inlet subcooling, the quench temperature (T_Q) increases with mass flux, while it decreases with local quality (x) as shown in Fig. 4. Figure 5 shows for a fixed G, T_Q increases with ΔT_{sub}, while it decreases with x. In general, the increase of G and ΔT_{sub} tends to increase heat transfer, thus rewet can occur at a higher temperature. The increase of x has an opposite effect resulting in lower T_Q. The pressure effect is shown in Fig. 6. For a fixed mass flux and inlet subcooling, the quench temperature increases with pressure. It is believed that the change in pressure causes the change of thermophysical properties which, in turn, affects heat transfer. Below 4 MPa, the effect of pressure increase to heat transfer is positive [6].

The length effect on the true quench temperature was studied in the 10,200 A run series—a special cold spot test series. The artificial cold spot spot was made of a bundle of fine copper wire wrapped tightly around the cold spot. The concept of an artificial cold spot is to create a thicker portion on the test tube, at which its electric resistance is less than the rest. Consequently, the cold spot has a cooler temperature than the rest, and true quench would initiate at the cold spot. True quench did occur at the cold spot, but for a rather narrow range of flow conditions. Outside this range, true quench never occurred at the cold spot.

To examine the length effect on the true quench temperature, a fixed mass flux was chosen first, and the same amount of local quality was generated at both locations of true quench in the cold spot test and in the regular test by adjusting inlet subcoolings. The two measured quench temperatures were then compared. The two locations of true quench should be quite distant.

Table 2 lists all six successful cold spot test results. Three additional regular runs are also included for the

Table 1. 10,300 Run series at $P = 344$ kPa

Run No.	G ($kg\ m^{-2}\ s^{-1}$)	ΔT_{sub} (°C)	Quench temperature (°C)	Quench location (cm)	H.F. due to direct heating at quench ($10^4 W\ m^{-2}$)	H.F. from BHP at quench ($10^5 W\ m^{-2}$)	x at quench location
10321	50	30	270	20	2.456	5.02	0.1366
10322	200	30	330	5	13.70	5.503	−0.0033
10323	300	30	341	5	15.60	5.36	−0.0219
10324	400	30	400	5	17.60	5.22	−0.0315
10325	50	20	250	30	1.218	4.87	0.1458
10326	100	20	285	20	2.80	4.85	0.0566
10327	200	20	307	5	7.90	4.84	0.0076
10328	300	20	343	5	11.60	4.697	−0.0076
10329	400	20	343	5	11.80	4.55	−0.0162
10330	50	10	220	50	0.766	4.70	0.1600
10331	100	10	236	30	1.539	4.52	0.0686
10332	200	10	248	25	2.145	4.18	0.0219
10333	300	10	245	30	3.663	4.035	0.0105
10334	400	10	260	30	5.578	3.89	0.0048

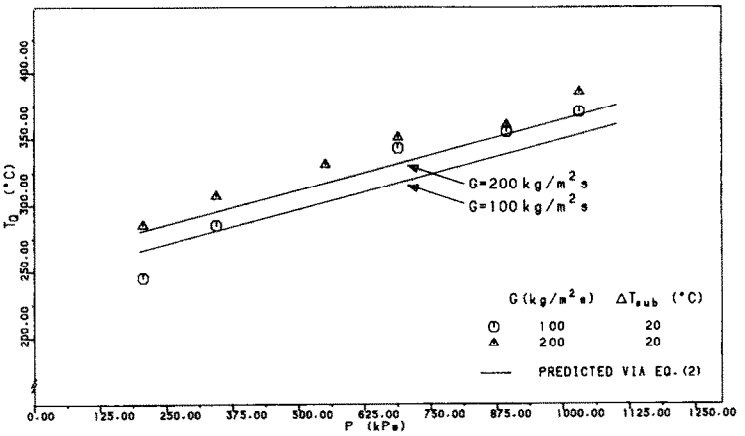

FIG. 6. Measured and predicted quench temperature vs pressure for fixed mass flux and inlet subcooling for 10,300 run series.

purpose of comparison. For example, in cold spot test run 10,205 A, true quench occurs at 15 cm from the BHP with x of 0.0351 and T_Q of 190°C. This compares with regular run 10,252, where true quench occurs at 30 cm with x of 0.0352 and T_Q of 195°C. These results indicate a very small effect on the true quench temperature particularly for quench location occurring at 15 cm away from the BHP. However, no clear conclusion can be drawn for true quench located very near the BHP. It is possible that the length effect is present at this region.

6. DISCUSSION

A successful run is defined by spontaneously collapsing vapour film, i.e. impulse cooling collapse, or sometimes dispersed flow rewet for the case of small mass flux and small inlet subcooling. Normally, no experimental run is accepted as a successful run when true quench is detected very near the bottom hot patch, (e.g. at thermocouple station located at 1 cm from the BHP). In this case, it is possible that true quench initiates at the BHP. However, for some runs when true quench is detected at the same location, the data may be accepted if the location of true quench temperature follows an expected trend.

After true quench occurs, the quench front propagates in both upstream and downstream directions. The two neighbouring thermocouples of the true quench thermocouple register slightly higher quench temperatures. This is referred to as the apparent quench temperature which is under a strong influence of axial conduction. A typical example is illustrated in Fig. 7, which indicates the true quench temperature, the apparent quench temperatures and the wall temperature at various locations at the time of true quench.

After studying the effects of parameters, an empirical correlation of the true quench temperature as a function of pressure, mass flux and inlet subcooling was derived as follows:

$$T_Q = 169.66 + 0.1050\,P + 0.1444\,G + 3.0347\,\Delta T_{sub}. \quad (2)$$

The coefficients of equation (2) were obtained from 10,300 run series with a total of 70 data points using the SPSS statistical package. The root mean square error of the correlation is 6.34%. Good agreement is observed between the correlation and the experimental data as shown in Figs 3–6.

In the literature, there is very little work published on

Table 2. Cold spot tests, 10,200A run series

Run No.	G (kg m^{-2} s^{-1})	ΔT_{sub} (°C)	Quench temperature (°C)	Quench location (cm)	H.F. due to direct heating at quench (10^4W m^{-2})	H.F. from BHP at quench (10^5W m^{-2})	x at quench location
10201 A	53	12	195	30*	2.031	2.70	0.0769
10202 A	53	6	200	30*	1.832	2.30	0.0731
10203 A	53	3	180	30*	1.082	2.20	0.0694
10211 A	53	16.5	210	15*	1.943	2.80	0.0610
10204 A	102	8	225	15*	1.947	2.60	0.0290
10205 A	102	2	190	15*	1.757	2.25	0.0351
10250	102	8	230	20	2.102	2.55	0.0301
10251	102	5.8	200	25	1.772	2.45	0.0339
10252	102	4	195	30	1.426	2.35	0.0352

*The location of cold spot from the BHP.

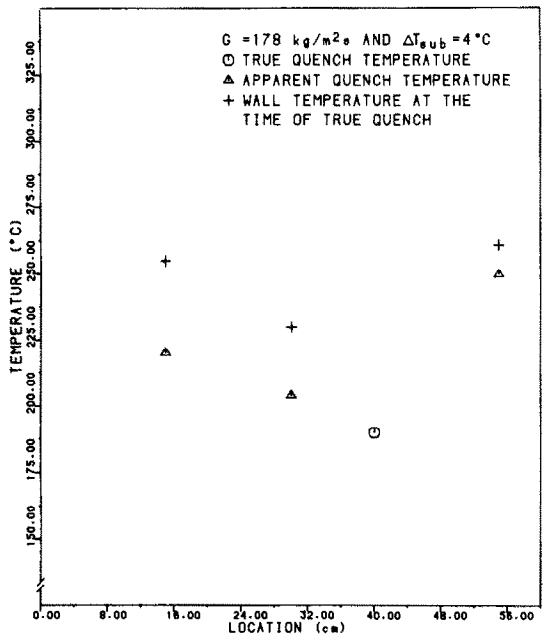

FIG. 7. True quench temperature and apparent quench temperatures at various locations for run 10,214.

true quench temperature measurements. Fung [11], and Groeneveld and Stewart [4] reported the first set of the true quench temperature data at atmospheric pressure and at high pressure, respectively. While they were performing film boiling experiments, occasionally they obtained some true quench temperature data at the termination of steady-state film boiling. Fung only obtained 12 data points from his experiments. Groeneveld and Stewart have produced more true quench temperature data, but at a much higher pressure range (2–9 MPa).

Comparing the present data with those of Fung's under similar inlet flow conditions (before the bottom hot patch), the true quench temperature in the present study is about 10% lower. It is due to different hot patch conditions [12]. The present experiment has a longer and hotter hot patch. Therefore, the enthalpy at the exit of the bottom hot patch is slightly higher. Higher enthalpy decreases heat transfer. Consequently, the present true quench temperature is lower.

Groeneveld and Stewart formulated a true quench temperature [4] based on their high pressure experimental data and Fung's low pressure data. They correlated the true quench temperature as a function of pressure and quality, i.e.

$x \leqslant 0$, $P < 9$ MPa

$$T_{min} = 284.7 + 44.11\,P - 3.72\,P^2 - \frac{x \times 10^4}{2.819 + 1.22\,P} \tag{3}$$

$x > 0$, $P < 9$ MPa

$$T_{min} = 284.7 + 44.11\,P - 3.72\,P^2 \tag{4}$$

where P is expressed in MPa.

Figure 8 presents a comparison of the present measured true quench temperature with Groeneveld and Stewart's correlation for $P = 206$ kPa. For $x < 0$, good agreement is observed. However, for $x > 0$, the present study shows T_Q varying from 216 to 285°C depending on mass flux and inlet subcooling in comparison with a constant high value of $T_{min} = 293.4$°C from the correlation. At a higher pressure of 550 kPa as shown in Fig. 9, overall agreement is good including the region of $x > 0$. Obviously, the present study shows that in certain regions T_Q depends not only on local quality, but also on mass flux and inlet subcooling.

Groeneveld and Stewart [4] compared several pool boiling type minimum film boiling correlations and Plummer's minimum film boiling correlation [13] with their true quench temperature data on a ΔT_{min} vs P basis. None of the correlations gave good prediction. Plummer's correlation is the only one based on forced

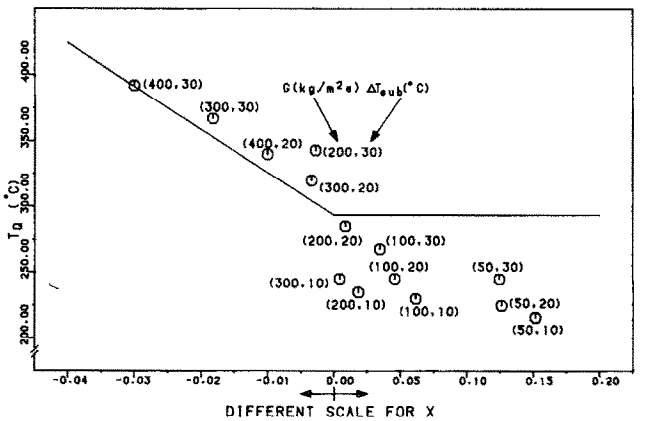

FIG. 8. Comparison of measured quench temperature with Groeneveld and Stewart's correlation for $P = 206$ kPa.

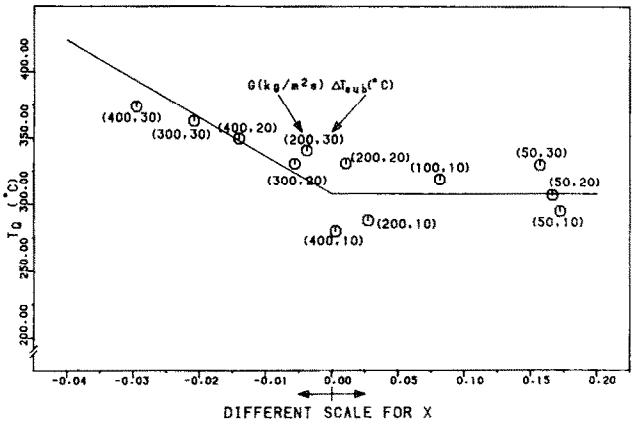

FIG. 9. Comparison of measured quench temperature with Groeneveld and Stewart's correlation for $P = 550$ kPa.

convective boiling including a mass flux effect. However, his data was obtained during transients with the presence of a rewetting front, which makes his correlation suspect.

7. CONCLUSIONS

(1) The true quench temperature is defined as the quench temperature at the onset of rewetting in a flow channel. It has two important features: (a) the onset of rewetting can occur anywhere along the flow channel, and (b) axial conduction is absent. The true quench temperature based on this study is a function of flow parameters.

(2) In general, the true quench temperature increases with mass flux, inlet subcooling and pressure, but decreases with increasing quality.

(3) An empirical correlation for the true quench temperature as a function of mass flux, pressure and inlet subcooling was formulated. The comparison between the correlation and the experimental data shows fair agreement.

(4) The present measured true quench temperature shows good agreement with Groeneveld and Stewart's correlation except in certain regions. At low pressure and positive local quality region, the present data shows that the true quench temperature depends not only on local quality but also on mass flux and inlet subcooling, while their correlation predicts a constant high value of true quench temperature.

(5) The true quench temperature is always lower than the apparent quench temperature.

(6) The true quench location tends to move toward the bottom hot patch as mass flux and inlet subcooling increase.

(7) Based on preliminary artificial cold spot tests, the length effect on the quench temperature is minimal, except when quench occurs very near the bottom hot patch.

(8) A properly functioning hot patch is strongly dependent on the method of soldering. An improper soldering process may cause the failure of the performance of the hot patch, i.e. the quench front initiates from the hot patch.

Acknowledgements—The authors wish to express their gratitude to the U.S. Nuclear Regulatory Commission and the Natural Sciences and Engineering Research Council of Canada for their financial support. The authors also extend thanks to Dr D. C. Groeneveld for his many valuable suggestions throughout the course of study.

REFERENCES

1. D. C. Groeneveld and S. R. M. Gardiner, A method of obtaining flow film boiling data for subcooled water, *Int. J. Heat Mass Transfer* **21**, 664–665 (1978).
2. K. K. Fung, S. R. M. Gardiner and D. C. Groeneveld, Subcooled and low quality film boiling of water at atmospheric pressure, *Nucl. Engng Des.* **55**, 51–57 (1979).
3. P. J. Berenson, Experiments on pool-boiling heat transfer, *Int. J. Heat Mass Transfer* **5**, 985–999 (1962).
4. D. C. Groeneveld and J. C. Stewart, The minimum film boiling temperature for water during film boiling collapse, *Proc. 7th Int. Heat Transfer Conf.*, Vol. 4, pp. 393–398, Munich, FR (1982).
5. O. C. Iloeje, D. N. Plummer, P. Griffith and W. M. Rohsenow, An investigation of the collapse and surface rewet in film boiling in forced vertical flow, *ASME Paper*, No. 73-WA/HT-20 (1973).
6. D. C. Groeneveld, Prediction methods for post-CHF heat transfer and superheated steam cooling suitable for reactor accident analysis, *TT/SETRE/82-4-E/DCGr*, Centre d'Etudes Nucléaires de Grenoble, France (1982).
7. E. K. Kalinin, S. A. Yarkho, I. I. Berlin, Y. S. Kochelaev and V. V. Kostyuk, Investigation of the crisis of film boiling in channels, two-phase flow and heat transfer in rod bundles, *Proc. ASME Winter Annual Meeting*, pp. 89–94, Los Angeles (1969).
8. S. C. Cheng, K. T. Poon, P. Lau, W. W. L. Ng and K. T. Heng, Transition boiling heat transfer in forced vertical flow (study of true quench temperature and construction of CHF table), Q. Rep. No. 23, ANLContract No. 31-109-38-5503 (1982).
9. F. F. Simon and R. J. Simoneau, Transition from film to nucleate boiling in vertical forced flow, *ASME Paper*, No. 69-HT-26 (1969).
10. P. W. K. Lau, Rewetting phenomena and measurements

of true quench temperature, M.A.Sc. Thesis, University of Ottawa, Canada (1983).
11. K. K. Fung, Subcooled and low quality film boiling of water in vertical flow at atmospheric pressure, Ph.D. Thesis, University of Ottawa, Canada (1981).
12. S. C. Cheng, K. T. Poon, P. Lau, K. T. Heng and W. W. L. Ng, Transition boiling heat transfer in forced vertical flow (study of true quench temperature and construction of CHF table), *Q. Rep.*, No. 24, ANL Contract No. 31-109-38-5503 (1982).
13. D. N. Plummer, O. C. Iloeje, P. Griffith and W. M. Rohsenow, A study of post critical heat flux heat transfer in a forced convection system, MIT Rep., No. 73645-80 (1973).

MESURE DES TEMPERATURES DE TREMPE VRAIE D'EAU SOUS-REFROIDIE DANS DES CONDITIONS DE CONVECTION FORCEE

Résumé—Une étude expérimentale est faite pour mesurer la température réelle de trempe en utilisant deux configurations pour fixer les fronts de trempe. On discute les effets des paramètres de débit massique (50–682 kg m^{-2} s^{-1}), de sous-refroidissement à l'entrée (2–30°C), de pression (101–1034 kPa) et de qualité locale (−0,0315–0,1990). On donne une formule de la température de trempe en fonction des paramètres, basée sur les présentes données expérimentales. Cette température mesurée est comparée avec celle disponible dans la bibliographie. Une série spéciale de spot froid est conduite pour examiner l'effet de la longueur sur la température de trempe.

MESSUNG DER TATSÄCHLICHEN QUENCH-TEMPERATUR VON UNTERKÜHLTEM WASSER BEI ERZWUNGENER KONVEKTION

Zusammenfassung—Eine experimentelle Untersuchung wurde durchgeführt, um die tatsächliche Quench-Temperatur zu messen. Als Parameter wurden untersucht: Die Massenstromdichte (im Bereich von 50–682 kg m^{-2} s^{-1}), die Unterkühlung am Eintritt (2–30°C), der Druck (101–1034 kPa) und der örtliche Dampfgehalt (−0,0315–0,1990). Aufgrund neuer Versuchsdaten wurde eine Beziehung der tatsächlichen Quench-Temperatur in Abhängigkeit von den Parametern formuliert. Die gemessene tatsächliche Quench-Temperatur wurde mit den in der Literatur verfügbaren Werten verglichen. Zur Untersuchung des Längeneinflusses auf die tatsächliche Quench-Temperatur wurde eine spezielle Versuchsreihe durchgeführt.

ИЗМЕРЕНИЯ ИСТИННОЙ ЗАКАЛОЧНОЙ ТЕМПЕРАТУРЫ НЕДОГРЕТОЙ ВОДЫ В УСЛОВИЯХ ВЫНУЖДЕННОЙ КОНВЕКЦИИ

Аннотация—Экспериментально измерена истинная закалочная температура с помощью двух нагретых участков, фиксирующих фронты закалки. Рассмотрены параметрические эффекты массового расхода (в диапазоне 50–682 кг $м^{-2}$ $с^{-1}$), недогрева на входе (2–30 С), давления (101–1,034 К Па) и локального паросодержания (−0,0315–0,1990). На основе проведенных экспериментов получена зависимость истинной закалочной температуры от параметров. Проведено сравнение измеренных значений с опубликованными в литературе данными. Выполнена специальная серия испытаний с холодным участком для исследования влияния его длины на истинное значение закалочной температуры.